

DOI: 10.1002/adma.200501617

Alignment of Carbon Nanotube Additives for Improved Performance of Magnesium Diboride Superconductors**

By Shi X. Dou,* Wai K. Yeoh, Olga Shcherbakova, David Wexler, Ying Li, Zhong M. Ren, Paul Munroe, Soo K. Chen, Kai S. Tan, Bartek A. Glowacki, and Judith L. MacManus-Driscoll

The rapid progress in developing MgB₂ superconductors since its relatively recent discovery^[1] has made this material a strong competitor to other low- and high-temperature superconductor (HTS) materials for technological applications, especially in niche markets such as magnetic resonance imaging (MRI). Thanks to the lack of weak links and the two-gap superconductivity of MgB₂,^[2,3] a number of different additives have been successfully used to enhance the critical current density, J_c , and the upper critical field, H_{c2} .^[4–12] Carbon nanotubes (CNTs) have unusual electrical, mechanical, and thermal properties,^[13–16] and hence are ideal components for inclusion in composites to improve composite performance. To take advantage of the extraordinary properties of CNTs, it is important to align the CNTs in the composites. Here, we report a method for aligning CNTs in CNT–MgB₂ superconductor composite wires through a readily scalable drawing technique. The aligned-CNT-doped MgB₂ wires show an enhancement in magnetic critical current density, $J_c(H)$, by more than one order of magnitude under high magnetic fields compared to the undoped samples. The CNTs also significantly improve heat transfer and dissipation. CNTs have mainly been used in structural materials, but here the advan-

tages of their use in functional composites are demonstrated, which has wider ramifications for other functional materials.

High in-field J_c of MgB₂ superconductors is a major requirement for large-scale applications. In addition, MgB₂ wires need to exhibit good mechanical properties and thermal stability. The additives studied so far have mainly been used to improve $J_c(H)$ by introducing effective pinning sites in MgB₂. Not much attention has been focused on the mechanical and thermal properties of the MgB₂ wire core. Among the additives that have been studied, CNTs have the potential to additionally improve the mechanical and thermal properties of the MgB₂ wires, since they have been used as reinforcing components in a number of different composites.^[17,18] Fosheim et al. have reported an enhanced flux pinning in Bi₂Sr₂CaCu₂O_{8+x} superconductors with embedded CNTs.^[19] Yang et al. have discovered a significant enhancement in $J_c(H)$ for HTSs by introducing nanorods as columnar pinning centers in the composites.^[20–22] We previously reported that CNT doping enhanced J_c under magnetic fields for bulk MgB₂.^[12,23] However, in that case the CNTs were randomly dispersed in bulk MgB₂. Inspired by the previous reports, in this communication we report a technique for aligning CNTs in Fe-sheathed MgB₂ wires. The advantages of doping with CNTs rather than other additives are: 1) Multiwalled CNTs can carry current densities up to 10⁹–10¹⁰ A cm⁻² (compared to a typical value of 10⁵–10⁶ A cm⁻² for superconductors), and remain stable for extended periods of time;^[14] CNT doping can thus improve the current path and connectivity between the grains in MgB₂. 2) The thermal conductivity for isolated multiwalled CNTs is estimated to be about 3000 W mK⁻¹,^[15] and hence could enhance heat dissipation and thermal stability of the MgB₂ wires. 3) Bundled CNTs have a very high axial strength and stiffness, approaching values for an ideal carbon fiber.^[16] If CNTs could be aligned along the longitudinal axis of the MgB₂ wires, it is expected that they would significantly improve the mechanical properties of the CNT–MgB₂ composite wire. 4) Finally, CNTs are one-dimensional (1D) materials with very large aspect ratios and can act as line-pinning sites instead of the point-defect-pinning sites provided by other additives. We demonstrate that a high degree of CNT alignment can be readily achieved by mechanical drawing in the powder-in-tube (PIT) process. The aligned CNT-doped MgB₂ wires show a significant enhancement in flux pinning and heat transfer.

Figure 1 shows $J_c(H)$ calculated from magnetization hysteresis loops with the magnetic field, H , applied both parallel

[*] Prof. S. X. Dou, W. K. Yeoh, O. Shcherbakova, Dr. D. Wexler
Institute for Superconducting and Electronic Materials
University of Wollongong
Northfields Ave., Wollongong, NSW 2522 (Australia)
E-mail: shi_dou@uow.edu.au

Dr. Y. Li, Z. M. Ren
Department of Materials Science and Engineering
Shanghai University
149 Yanchang Rd., Shanghai 200072 (P.R. China)

Prof. P. Munroe
Electron Microscope Unit
University of New South Wales
Sydney, NSW 2000 (Australia)

S. K. Chen, K. S. Tan, Dr. B. A. Glowacki,
Dr. J. L. MacManus-Driscoll
Department of Materials Science and Metallurgy
University of Cambridge
Pembroke St., Cambridge CB2 3QZ (UK)

[**] This work was supported by the Australian Research Council, Hyper Tech Research Inc. (Columbus, OH), and Alphatech International Ltd. (New Zealand). W. K. Yeoh received an Australia–Asia Award funded by the Australian Government. Z. M. Ren and Y. Li thank the Natural Science Foundation of China for support under grants Nos. 59 871 026, 50 225 416, and 50 234 020. K. S. Tan received support from the ORS/Cambridge Commonwealth Trust. Funding from EPSRC in the UK is also acknowledged.

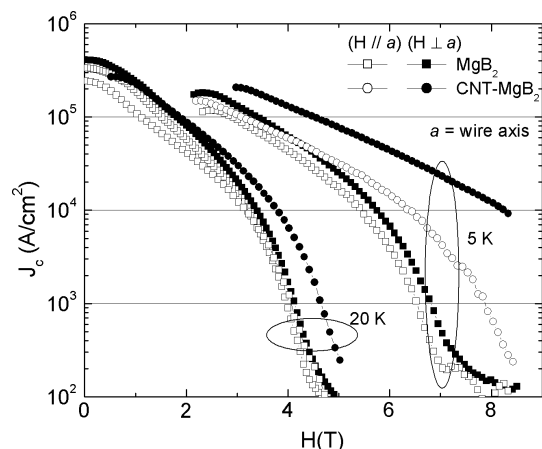


Figure 1. Magnetic critical current density as a function of the applied magnetic field at 5 K and 20 K for the undoped and CNT-doped MgB₂ wires processed at 800 °C for 30 min. All the samples used for the magnetic measurements have the same dimensions: an outer diameter of 0.7 mm and a length of 2.7 mm. The measurement field H was applied perpendicular and parallel to the wire axis, a , during the measurement of M – H loops.

and perpendicular to the wire axis, a , for both undoped and CNT-doped MgB₂ wires. It is noted that for the undoped MgB₂ wire, there is a small difference in $J_c(H)$ along the two measured field directions due to the wire-drawing process. In contrast, for CNT-doped MgB₂, $J_c(H)$ shows two characteristic features: a strong anisotropy with regards to the field direction, and a clear enhancement of flux pinning in the high-field region, as compared to the undoped sample. The anisotropy in magnetic J_c is stronger at 5 K than at 20 K, and the extent of this anisotropy increases with the magnetic field H , ranging from a factor of 2–3 under low fields to more than one order of magnitude under high fields. The enhancement in $J_c(H)$ performance due to CNT doping is more significant at low temperatures and under higher fields. For example, the magnetic J_c in the $H \perp$ direction increases by a factor of 4 at 20 K and 4 T, and by a factor of 37 at 5 K and 7 T, as a result of CNT doping. What is more striking is that the enhancement in J_c for the CNT-doped MgB₂ wires occurs with the applied field H both parallel and perpendicular to the wire axis. $J_c(H \perp a)$, perpendicular to the wire axis, shows more significant enhancement than $J_c(H \parallel a)$, parallel to the wire axis, compared to the undoped MgB₂ wire.

X-ray diffraction (XRD) and electron diffraction patterns do not show any evidence for a preferred crystalline orientation of MgB₂ grains in the wire core in either longitudinal or transverse directions relative to the wire axis. This is not surprising since the MgB₂ crystal is formed by an in-situ process in which there is no driving force for MgB₂ crystalline alignment. Thus, the anisotropy measured above is not due to MgB₂ crystallite alignment. Figure 2a shows a scanning electron microscopy (SEM) image of the CNT-doped MgB₂ wire. A strongly elongated macrostructure is clearly evident along the wire axis. In the CNT-doped bulk material, the CNTs are randomly dispersed in the MgB₂ matrix, and most of the

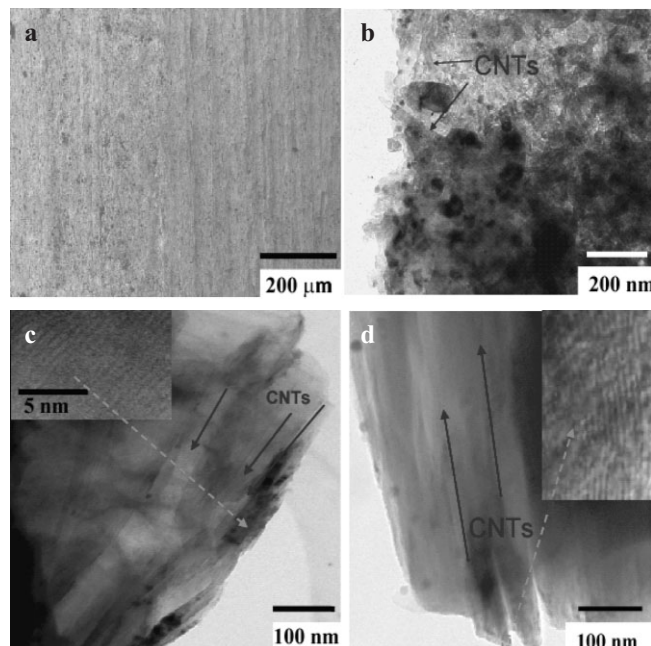


Figure 2. a) Focused-ion-beam-SEM microscopy image of the CNT-doped MgB₂ wire core showing the elongated macrostructure along the wire axis; b) Transmission electron microscopy (TEM) image of the CNT-doped MgB₂ pellet showing the entangled CNTs randomly distributed in the MgB₂ matrix; c) TEM image of the CNT-doped MgB₂ wire showing a bundle of CNTs aligned in the same direction in the MgB₂ matrix. The inset in (c) is a high-resolution image of one of the CNTs. d) TEM image of several parallel CNTs embedded in MgB₂. The inset in (d) is a high-resolution lattice image of one of the CNTs.

CNTs are highly entangled, as shown in Figure 2b. In contrast, for the PIT process, the mixture of Mg and B powder and the CNT additives flow along the wire axis as a result of continuing drawing and reduction processes. The drawing process is repeated more than thirty times to reduce the iron sheath/Mg + B powder composite from 10 mm in diameter to 1–1.4 mm in diameter. Because of the high aspect ratio of CNTs, the drawing force leads the entangled CNTs to straighten in the longitudinal direction. The degree of CNT alignment increases with an increased number of drawings. For a single-filament MgB₂ wire, the filament diameter is relatively large compared to the CNTs. However, practical conductors are made of multiple filaments with the diameter of each filament being as small as 10 μm, which is comparable to the diameter of the CNTs (up to 2 μm). Thus, a high degree of CNT alignment can be achieved. Nevertheless, the extent of CNT alignment is clearly evident from both magnetic J_c measurements and transmission electron microscopy (TEM) observations of single-core filaments. Figure 2c shows a TEM image of embedded, straightened CNTs aligned in the same direction in the MgB₂ wire core. The inset shows a high-resolution image of the lattice of one of the CNTs. Figure 2d also shows a TEM image for several parallel CNTs embedded in the MgB₂ matrix. The inset in Figure 2d shows the high-resolution lattice image of one of the CNTs. These results indicate that the anisotropy in J_c originates from the alignment of CNTs during

the mechanical drawing process. The CNT-induced anisotropy in J_c is attributable to two factors: high axial conductivity^[14,24] and the large aspect ratio of the CNTs. The CNTs aligned along the core axis are expected to improve the connectivity between grains by bridging poorly connected regions, which helps to overcome an ubiquitous problem for the in-situ reaction process, since the density of MgB₂ only reaches about 50 % of the theoretical density for wires fabricated by this process. The better in-field J_c performance in the longitudinal direction, when the field is applied perpendicular to the wire axis, suggests that the presence of CNTs in the longitudinal direction induces strong pinning sites transverse to the longitudinal axis. This comes as a surprise as we expect exactly the opposite behavior, that is, stronger pinning should occur along the longitudinal direction of the CNTs when the field is applied parallel to the wire axis, since the flux lines are expected to have a strong interaction with the CNTs. However, we must consider that when the CNTs are aligned along the wire axis, the total cross-sectional area of the CNTs transverse to the wire axis is much smaller than in the longitudinal direction due to the high aspect ratio of the CNTs. Thus, the overall interaction between the CNTs and the flux lines is stronger when the field is applied perpendicular to the longitudinal wire axis rather than parallel to the wire axis, and hence the J_c in the longitudinal direction shows better in-field performance than in the transverse direction. As reported previously, the enhancement in J_c by CNTs can be attributed to two factors: carbon substitution for B and the role of CNTs as strong pinning centers.^[12,23]

Furthermore, the CNTs have a strong effect on heat transfer during materials processing due to their high thermal conductivity. Figure 3a shows the effect of the heating rate on $J_c(H)$ behavior for the pure and CNT-doped MgB₂ wires. We note that the heating rate has no effect on $J_c(H)$ for the CNT-doped MgB₂ wire, while $J_c(H)$ for the pure MgB₂ wire processed at a rapid heating rate of 15 °C min⁻¹ is lower than that

at a slow heating rate of 1.7 °C min⁻¹ by a factor of three. In the rapid heating case, for the pure MgB₂ wire, the solid-state reaction is inhomogeneous due to the large temperature gradient. On the other hand, the CNTs, because of their efficient heat-transfer properties and by acting as nucleation centers, mediate a homogeneous reaction throughout the core. For the slow heating case, there is sufficient time for heat transfer to the interior, and hence the reaction can take place homogeneously in the entire core region. This interpretation is further verified by the differential thermal analysis (DTA) plots for the Fe-sheathed pure MgB₂ and 10 % CNT-doped MgB₂ wires with a heating rate of 15 °C min⁻¹, as shown in Figure 3b. There are two exothermic peaks for the pure MgB₂ wires, while for the CNT-doped MgB₂ wires, these two peaks are merged into one broad peak. The first peak is due to the reaction between Mg and B₂O₃, while the second peak is attributable to the formation of MgB₂.

CNTs, because of their high aspect ratio, are desirable nucleation centers for triggering and propagating MgB₂ formation along their entire length. Since the CNTs have a high thermal conductivity, heat is transferred along the CNTs to the adjacent regions. Thus, the MgB₂ formation reaction takes place with the CNTs as the nucleation centers and propagates along the length of the CNTs. The high thermal conductivity and desirable elongated geometry of the CNTs is responsible for the insensitivity of CNT-doped MgB₂ wires to the heating rate, which is convenient and advantageous for the manufacture of practical conductors.

In summary, the alignment of CNTs in CNT-MgB₂ composite wires has been achieved by a readily scalable drawing technique. The aligned CNT-doped MgB₂ wires show an enhancement of the magnetic J_c by more than an order of magnitude under high-field conditions. The aligned CNTs induce anisotropy in magnetic J_c with respect to the direction of the applied field and significantly improve heat transfer and dissipation during materials processing. In addition to the benefits of the

electrical and thermal conductivity of CNT doping, the alignment of CNTs along the wire axis is expected to lead to enhancements of mechanical properties such as tensile strength and flexibility due to the unique axial strength of CNTs. Studies on these properties are underway.

Experimental

CNT-doped MgB₂ wires were prepared using the PIT method through an in-situ reaction process [25,26]. Powders of magnesium (99 %) and amorphous boron (99 %) were well mixed with 0 and 10 wt.-% randomly distributed multiwalled carbon nanotubes (outer diameter (OD): 20–30 nm, length: 0.5–2 μm) and thoroughly ground. An ultrasonic mixer was used to improve the homogeneity of the mixed Mg, B, and CNTs.

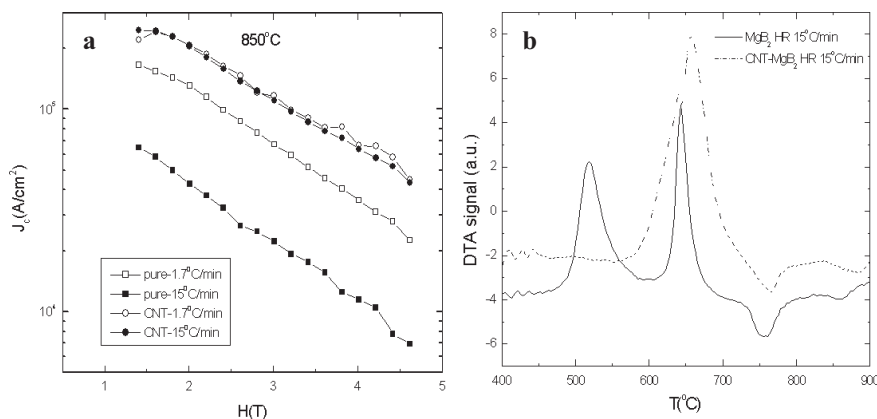


Figure 3. a) A comparison of $J_c(H)$ for the undoped and CNT-doped MgB₂ wires processed at heating rates of 100 °C h⁻¹ and 900 °C h⁻¹. The heating rate has no effect on $J_c(H)$ for CNT-doped MgB₂ wires, but the fast heating rate severely degrades $J_c(H)$ in the undoped sample. b) Differential thermal analysis (DTA) curves for the undoped and CNT-doped MgB₂ wires processed at a heating rate of 15 °C min⁻¹.

The Fe tube had an OD of 10 mm and a wall thickness of 1 mm, and was 10 cm long with one end of the tube sealed. The mixed powder was filled into the tube and the remaining end was blocked using an aluminum bar. The composite was drawn to a 1–1.4 mm diameter wire through a series of more than 30 dies with a reduction rate of about 10% in every drawing. For fabrication of multifilament wires, a bundle of single-core wires was inserted into an iron tube, and the composite was drawn into a 1–1.4 mm diameter wire. Several short samples, 2 cm in length, were cut from the wire. These pieces were then sintered in a tube furnace at 800 and 830 °C for 30 min at a heating rate of 3 °C min⁻¹, and finally furnace-cooled to room temperature. A high-purity argon gas flow was maintained throughout the sintering process. An undoped sample was also made under the same conditions for use as a reference sample. Sintering of wires at different heating rates was carried out at Cambridge. Two heating rates of 1.7 and 15 °C min⁻¹ were used, followed by isothermal annealing at 850 °C for 30 min. The samples were then furnace-cooled to room temperature. The phase and crystal structures of all the samples was obtained from XRD patterns measured using a Philips (PW1730) diffractometer with Cu K α radiation. DTA was performed to study the effect of the heating rate on J_c . The grain morphology and microstructure were also examined by an SEM equipped with a focused ion beam (FIB) apparatus and by TEM. The magnetization was measured at 5 and 20 K using a Physical Property Measurement System (PPMS, Quantum Design) in a time-varying magnetic field with a sweep rate of 50 Oe s⁻¹ (1 Oe = 10³/4 π A m⁻¹) and an amplitude of 8.5 T. Bar-shaped samples with a diameter of 0.7 mm and length of 2.7 mm were cut from the wire core for magnetic measurements. The magnetic measurements were performed by applying a magnetic field perpendicular and parallel to the wire sample axis. Since there is a large sample-size effect on the magnetic J_c for MgB₂ [27,28], all the samples measured were of the same size. The magnetic J_c was derived from the width of the magnetization loop using Bean's model. J_c versus magnetic field was measured up to 8.5 T.

Received: August 3, 2005

Final version: November 14, 2005

Published online: February 22, 2006

- [1] J. Nagamatsu, N. Nakagawa, T. Muranaka, Y. Zenitani, J. Akimitsu, *Nature* **2001**, *410*, 63.
- [2] D. C. Larbalestier, L. D. Cooley, M. O. Rikel, A. A. Polyanskii, J. Jiang, S. Patnaik, X. Y. Cai, D. M. Feldmann, A. Gurevich, A. A. Squitieri, M. T. Naus, C. B. Eom, E. E. Hellstrom, R. J. Cava, K. A. Regan, N. Rogado, M. A. Hayward, T. He, J. S. Slusky, P. Khalifah, K. Inumaru, M. Haas, *Nature* **2001**, *410*, 186.
- [3] A. Gurevich, *Phys. Rev. B: Condens. Matter Mater. Phys.* **2003**, *67*, 184515.
- [4] J. Wang, Y. Bugoslavsky, A. Berenov, L. Cowey, A. D. Caplin, L. F. Cohen, J. L. MacManus-Driscoll, L. D. Cooley, X. Song, D. C. Larbalestier, *Appl. Phys. Lett.* **2002**, *81*, 2026.
- [5] S. X. Dou, S. Soltanian, J. Horvat, X. L. Wang, S. H. Zhou, M. Ionescu, H. K. Liu, P. Munroe, M. Tomsic, *Appl. Phys. Lett.* **2002**, *81*, 3419.
- [6] R. H. T. Wilke, S. L. Bud'ko, P. C. Canfield, D. K. Finnemore, R. J. Suplinskas, S. T. Hannahs, *Phys. Rev. Lett.* **2004**, *92*, 217003.
- [7] V. Braccini, A. Gurevich, J. E. Giенcke, M. C. Jewell, C. B. Eom, D. C. Larbalestier, A. Pogrebnyakov, Y. Cui, B. T. Liu, Y. F. Hu, J. M. Redwing, Q. Li, X. X. Xi, R. K. Singh, R. Gandikota, J. Kim, B. Wilkens, N. Newman, J. Rowell, B. Moeckly, V. Ferrando, C. Tarantini, D. Marré, M. Putti, C. Ferdeghini, R. Vaglio, E. Haanappel, *Phys. Rev. B: Condens. Matter Mater. Phys.* **2004**, *71*, 012504.
- [8] H. Kumakura, H. Kitaguchi, A. Matsumoto, H. Hatakeyama, *Appl. Phys. Lett.* **2004**, *84*, 3669.
- [9] S. X. Dou, V. Braccini, S. Soltanian, R. Klie, Y. Zhu, S. Li, X. L. Wang, D. Larbalestier, *J. Appl. Phys.* **2004**, *96*, 7549.
- [10] M. D. Sumption, M. Bhatia, M. Rindfleisch, M. Tomsic, S. Soltanian, S. X. Dou, E. W. Collings, *Appl. Phys. Lett.* **2005**, *86*, 092507.
- [11] A. Matsumoto, H. Kumakura, H. Kitaguchi, H. Hatakeyama, *Supercond. Sci. Technol.* **2003**, *16*, 926.
- [12] S. X. Dou, W. K. Yeoh, J. Horvat, M. Ionescu, *Appl. Phys. Lett.* **2003**, *83*, 4996.
- [13] R. H. Baughman, A. A. Zakhidov, W. A. de Heer, *Science* **2002**, *297*, 787.
- [14] B. Q. Wei, R. Vajtai, P. M. Ajayan, *Appl. Phys. Lett.* **2001**, *79*, 1172.
- [15] P. Kim, L. Shi, A. Majumdar, P. L. McEuen, *Phys. Rev. Lett.* **2001**, *87*, 215502.
- [16] M. M. J. Treacy, T. W. Ebbesen, J. M. Gibson, *Nature* **1996**, *381*, 678.
- [17] Y. Li, I. A. Kinloch, A. H. Windle, *Science* **2004**, *304*, 276.
- [18] E. S. Choi, J. S. Brooks, D. L. Eaton, M. S. Al-Haik, M. Y. Hussaini, H. Garmestani, D. Li, K. Dahmen, *J. Appl. Phys.* **2003**, *94*, 6034.
- [19] K. Fossheim, E. D. Tuset, T. W. Ebbesen, M. M. J. Treacy, J. Schwartz, *Phys. C (Amsterdam, Neth.)* **1995**, *248*, 195.
- [20] P. Yang, C. M. Lieber, *Science* **1996**, *273*, 1836.
- [21] P. Yang, C. M. Lieber, *Appl. Phys. Lett.* **1997**, *70*, 3158.
- [22] P. Yang, C. M. Lieber, *J. Mater. Res.* **1997**, *12*, 2981.
- [23] W. K. Yeoh, J. Horvat, S. X. Dou, V. Keast, *Supercond. Sci. Technol.* **2004**, *17*, S572.
- [24] S. Frank, P. Poncharal, Z. L. Wang, W. A. de Heer, *Science* **1998**, *280*, 1744.
- [25] S. X. Dou, J. Horvat, S. Soltanian, X. L. Wang, M. J. Qin, S. H. Zhou, H. K. Liu, P. Munroe, *IEEE Trans. Appl. Supercond.* **2003**, *13*, 3199.
- [26] S. Soltanian, X. L. Wang, I. Kusevi, E. Babi, A. H. Li, M. J. Qin, J. Horvat, H. K. Liu, E. W. Collings, E. Lee, M. D. Sumption, S. X. Dou, *Phys. C (Amsterdam, Neth.)* **2001**, *361*, 84.
- [27] M. J. Qin, S. Keshavarzi, S. Soltanian, X. L. Wang, H. K. Liu, S. X. Dou, *Phys. Rev. B: Condens. Matter Mater. Phys.* **2004**, *69*, 012507.
- [28] J. Horvat, S. Soltanian, X. L. Wang, S. X. Dou, *Appl. Phys. Lett.* **2004**, *84*, 3109.